Int. J. Heat Mass Transfer. Vol. 24, No. 7, pp. 1171–1177, 1981
Printed in Great Britain

0017-9310/81/071171-07 $02.00/0

COUPLING OF HEAT TRANSFER BETWEEN TWO NATURAL CONVECTION SYSTEMS SEPARATED BY A VERTICAL WALL

R. VISKANTA and D. W. LANKFORD

Heat Transfer Laboratory, School of Mechanical Engineering, Purdue University, West Lafayette, IN 47907, U.S.A.

(*Received* 16 *September* 1980 *and in revised form* 6 *January* 1981)

Abstract—This paper considers the problem of thermal coupling by conduction through a wall separating two fluid reservoirs at different temperatures. A simple analysis is presented to predict heat transfer between two natural convection systems separated by a wall. Also, experiments have been performed in a test apparatus capable of simultaneous optical observation of the two laminar boundary layers using a Mach–Zehnder interferometer. Air at atmospheric pressure and near room temperature was used as the test fluid. Reasonably good agreement between the predictions and the experimental data was obtained. It is also shown that the current accepted procedure for predicting overall heat transfer coefficient by neglecting the thermal interaction between the two natural convection systems separated by a wall is appropriate for ordinary fluids.

NOMENCLATURE

- b, plate (wall) thickness;
- C, coefficient in equation (2);
- g, gravitational constant;
- L, length of plate;
- M, dimensionless parameter defined by equation (6);
- Nu_x, local Nusselt number, hx/k;
- P, dimensionless parameter defined by equation (7);
- Pr, Prandtl number, ν/α;
- q, local heat flux;
- q^*, dimensionless heat flux, $q/(k_w/b)(T_{1\infty} - T_{2\infty})$;
- Ra, Rayleigh number, $Ra = GrPr = g\beta(T_{1\infty} - T_{2\infty})L^3/\nu\alpha$;
- Ra_{x_1}, local Rayleigh number, $Ra_x = Gr_x \cdot Pr = g\beta(T_w - T_\infty)x^3/\nu\alpha$;
- U, overall heat transfer coefficient, $g/(T_{1\infty} - T_{2\infty})$;
- x, coordinate measured along the plate [Fig. 1(b)];
- y, coordinate measured perpendicular to the plate [Fig. 1(b)].

Greek symbols

- α, thermal diffusivity;
- β, thermal expansion coefficient;
- θ_{iw}, dimensionless temperature, $|T_{wi} - T_{i\infty}|/(T_{1\infty} - T_{2\infty})$;
- ξ, dimensionless distance measured along the plate, x/L.

Subscripts

- 1, refers to fluid 1;
- 2, refers to fluid 2;
- ∞, refers to free stream;
- w, refers to the wall.

INTRODUCTION

A VERY common problem encountered in various applications is the prediction of the heat exchange rate between two fluid streams separated by a wall. Three limiting situations are possible: forced convection on both sides; forced convection on one side and natural convection on the other; and natural convection on both sides. Examples of systems where such situations are encountered include heat exchange equipment, cooling of electronic components, fluid filled containers, habitable space and numerous others. It is an accepted engineering practice in design calculations to use the concept of the overall heat-transfer coefficient and break down the general problem into one of determining the individual thermal resistances to heat transfer in the two convective systems together with that of the intermediate wall [1]. Implicit in this type of approach is the assumption that the convective heat-transfer coefficients (conductances) can be determined for boundary conditions appropriate for the problem at hand. These conditions are frequently taken to be that of uniform wall temperature or of uniform heat flux. However, neither the heat-transfer coefficients nor the variation of the temperature along the sides of the wall are known since both depend on the heat-transfer rate (which is the quantity being determined).

It is recognized that neither the constant wall temperature nor the constant heat flux boundary condition apply accurately when heat is transferred between two fluid streams separated by a wall. Yet this type of a heat-transfer situation has received relatively little previous attention. Heat exchange between two fluids separated by a wall in a duct [2, 3], forced convection [4, 5], and natural convection [6] boundary layer flows have been studied. However, the accuracy and the conditions for which the simplified approach for predicting heat exchange between two fluid streams separated by a wall [1] has rarely been

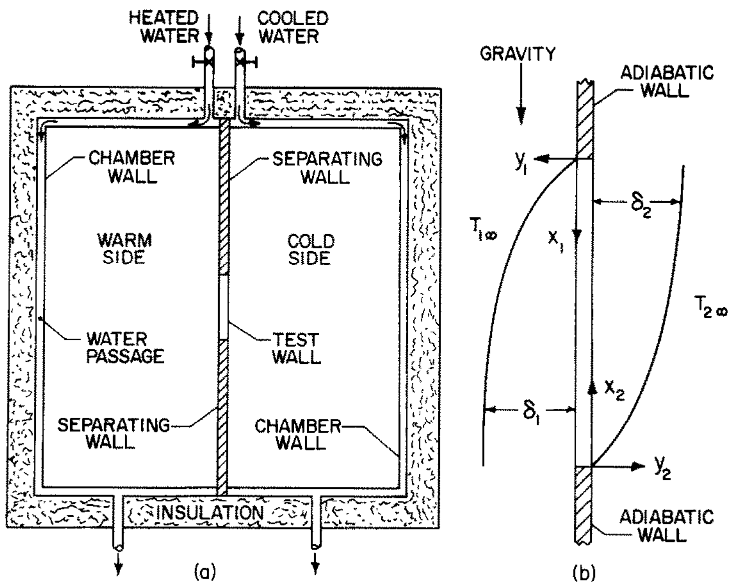

FIG. 1. Schematic diagram of the test cell and coordinate system of physical model.

subjected to a very rigorous analysis or experimental validation. Also, in analogous mass-transfer operations, the practice of adding interphase resistances in defining the overall mass-transfer coefficient is not always valid [7].

This paper gives consideration to the coupling of heat transfer between two natural convection systems separated by a heat conducting wall. Experiments were performed and a simple analysis developed to predict the extent of the thermal interaction between the two fluid streams. The experiments were conducted with air in natural convection systems and comparisons made with the predictions of heat transfer through the wall made by commonly accepted procedures in the heat-transfer literature (for the purpose of establishing the validity of these approaches).

EXPERIMENTS

Test apparatus

A schematic diagram of the test cell is shown in Fig. 1(a). The cell consisted of a double-wall chamber which was divided into two equal parts by a vertical wall. The inside dimensions of each chamber were 70 cm high by 34 cm wide by 38 cm deep. The temperature of each chamber was controlled independently by circulating water from a constant temperature bath through the double walls of the chamber. Provisions were made to distribute the water evenly over the top and sides of the chamber and to insure uniform wall temperatures. The two chambers were separated from each other by a 0.635 cm thick balsa-wood sheet. A 10.16 cm high by 0.635 cm thick test wall was positioned in the center of the chamber, mounted between the two adiabatic walls (balsa sheets), and spanned the entire depth of the chamber. A 6.8 cm radius viewing port was constructed on the front and back sides of the chamber for optical observation of the environment on both sides of the vertical plane. Optical quality windows were attached to the sides of the chamber and covered the viewing ports. The entire chamber was covered with a 5 cm thick fiberglass insulation, with the insulation over the viewing ports being removable.

A Mach–Zehnder interferometer, of conventional rectangular design and having 25 cm dia. optics, was used for measuring the temperature distribution. A He–Ne laser served as a light source, and a system of lenses, along with a 25 cm dia. parabolic mirror, produced a collimated beam.

Numerous thermocouples were mounted at various locations on the test plate, inside the chamber, and on the chamber walls for measuring temperatures. Three thermocouples were mounted 7.62 cm from the back of each chamber wall, centered horizontally and located at heights of 15.24, 27.94 and 45.72 cm from the top. Two thermocouples, centred vertically, were located 10.16 cm from each end on both sides of the test plate. Three thermocouples, placed 6.35 cm away from the plate, centered vertically and spaced 7.62 cm apart on both sides of the plate, measured the 'free stream' reference temperature of the fluid. Three additional thermocouples were mounted 5 cm from the vertical chamber walls and were located 15, 28 and 46 cm from the bottom of the chamber.

Procedure and data reduction

The interferometer was adjusted so that the virtual focal point of the recombined beams was at the center of the test cell and a horizontal fringe pattern was produced. Water, at desired temperatures, was circulated through the chamber from the constant temperature bath. Temperature readings were taken at predetermined time intervals and the interference fringe patterns were photographed with a Polaroid (model 180) camera to check if steady-state conditions were reached. Depending on the temperatures in the chamber, it took about 12 h to reach steady-state conditions. At that time thermocouple readings were recorded and interference fringe patterns were photographed.

Air at atmospheric pressure was the test fluid in both of the chambers. Three different materials: glass, brass and copper, covering a wide range of thermal conductivities, were used for the vertical separating wall. Several different tests were performed for each wall and the temperature differences between the chambers ranged between about 10 and 40°C.

The interference fringe patterns photographed were interpreted using a LTD Vernier Microscope. The reference temperatures needed to interpret the interferograms were obtained from the readings of the calibrated thermocouples. The local heat-transfer coefficients (averaged along the test beam) were determined by following the procedure suggested in the literature [8].

ANALYSIS

The physical model and coordinate system are shown schematically in Fig. 1(b). A warmer fluid at temperature $T_{1\infty}$, say, on the left-hand side is separated from a colder fluid at temperature $T_{2\infty}$, on the right-hand side by a heat conducting wall. Heat conduction across the wall will produce natural convection in the two systems. The analysis is restricted to the case after steady-state conditions have been reached. It is assumed that the flow is laminar and that physical properties, except the density in the buoyancy term, are constant. The problem can be formulated in terms of the boundary layer equations for the two systems and then coupling the equations through energy balances at the two faces of the wall [4–6]. Instead a simpler and more direct approach will be presented.

If heat conduction along the plate is neglected, in comparison to transverse heat conduction, under steady-state conditions we have

$$-k_1 \left.\frac{\partial T_1}{\partial y_1}\right|_{y_1=0} = \left(\frac{k_w}{b}\right)[T_{w2}(x_2) - T_{w1}(x_1)] = k_2 \left.\frac{\partial T_2}{\partial y_2}\right|_{y_2=0}. \quad (1)$$

For laminar natural convection from a vertical plate the heat fluxes $q_1(x_1)$ and $q_2(x_2)$ at the two surfaces can be expressed as [9]

$$q_1(x_1) = C(Pr_1)k_1\left(\frac{g\beta_1 Pr_1}{v_1^2}\right)^{1/4} \times \frac{[|T_{w1}(x_1)-T_{1\infty}|]^{5/3}}{\left\{\int_0^{x_1}[|T_{w1}(s)-T_{1\infty}|]^{5/3}\,ds\right\}^{1/4}} \quad (2)$$

and

$$q_2(x_2) = C(Pr_2)k_2\left(\frac{g\beta_2 Pr_2}{v_2^2}\right)^{1/4} \times \frac{[T_{w2}(x_2)-T_{2\infty}]^{5/3}}{\left\{\int_0^{x_2}[T_{w2}(s)-T_{2\infty}]^{5/3}\,ds\right\}^{1/4}} \quad (3)$$

respectively. For laminar free convection an accurate expression for the constant $C(Pr)$ is given by Churchill and Ozoe [10].

In terms of dimensionless variables equations (1)–(3) can be written as

$$1-\theta_{1w}(\xi_1)+\theta_{2w}(\xi_2) = C_1(Pr_1)\left(\frac{k_1}{k_w}\right)\left(\frac{b}{l}\right)Ra_1^{1/4} \times \theta_{1w}^{5/3}(\xi_1)\left[\int_0^{\xi_1}\theta_{1w}^{5/3}(\eta)\,d\eta\right]^{-1/4} \quad (4)$$

and

$$C_1(Pr_1)\left(\frac{k_1}{k_w}\right)\left(\frac{b}{L}\right)Ra_1^{1/4}\,\theta_{1w}^{5/3}(\xi_1)\left[\int_0^{\xi_1}\theta_{1w}^{5/3}(\eta)d\eta\right]^{-1/4} = q^* = C_2(Pr_2)\left(\frac{k_2}{k_w}\right)\left(\frac{b}{L}\right)Ra_2^{1/4}\,\theta_{2w}^{5/3}(\xi_2) \times\left[\int_0^{\xi_2}\theta_{2w}^{5/3}(\eta)d\eta\right]^{-1/4}. \quad (5)$$

Note that from the coordinate system selected [see Fig. 1(b)], the dimensionless distance $\xi_1 = 1 - \xi_2$. Inspection of equations (4) and (5) reveals that the wall temperatures $\theta_{1w}(\xi_1)$ and $\theta_{2w}(\xi_2)$ depend on two parameters

$$P = (k_1/k_w)(b/L)\,Ra_1^{1/4} \quad (6)$$

and

$$M = (k_1/k_2)(Ra_1/Ra_2)^{1/4}. \quad (7)$$

An exact analytical solution of equations (4) and (5) does not appear feasible; and therefore a numerical solution was sought. The dimensionless wall temperatures at discrete N positions were approximated by discrete functions [5], and the expressions substituted into equations (4) and (5). The resulting system of $2N$ nonlinear algebraic equations were then solved for the $2N$ unknown functions. Unfortunately, the large number (ranging from 80 to 200) of nonlinear equations resulted in convergence difficulties, and the method had to be abandoned. The numerical solution of equations (4) and (5) was obtained by iteration using 20, 40 and 100 intervals $\Delta\xi_1$ for ξ_1 between 0 and 1. The results reported have been obtained with 100 intervals, but they differed at most in the third significant figure from those obtained using only 40 intervals.

Once the wall temperature distributions $\theta_{1w}(\xi_1)$ and $\theta_{2w}(\xi_2)$ have been determined, the heat flux $q_1^*(\xi_1) = q_1^*(\xi_2) = q^*(\xi_1)$ can be computed from equations (2) and (3). The local Nusselt number on side 1, Nu_{x_1}, can be expressed, for example, as

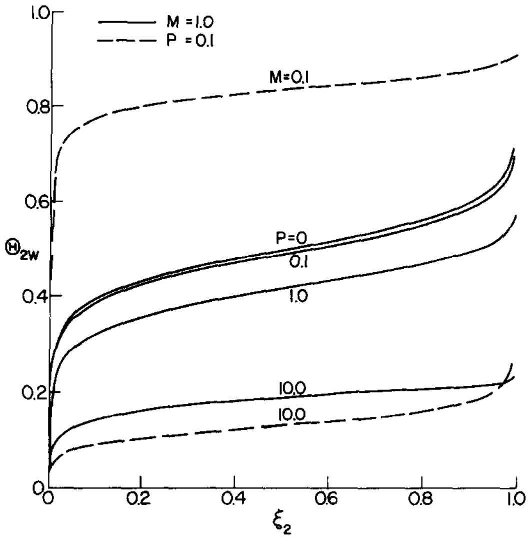

FIG. 2. Effect of parameters P and M on dimensionless wall temperature variation along the wall, $Pr_1 = Pr_2 = 0.708$.

$$\frac{Nu_{x_1}}{Ra_{x_1}^{1/4}} = \frac{q^* \xi_1^{1/4}}{\left(\frac{k_1}{k_w}\right)\left(\frac{b}{L}\right) Ra_1^{1/4} \theta_{1w}^{5/4}}. \tag{8}$$

The overall heat transfer coefficient can be written in dimensionless form as

$$q^* = \frac{Ub}{k_w} = \left\{ \left[\left(\frac{k_1}{k_w}\right)\left(\frac{b}{x_1}\right) Nu_{x_1}\right]^{-1} + 1 + \left[\left(\frac{k_2}{k_w}\right)\left(\frac{b}{x_2}\right) Nu_{x_2}\right]^{-1} \right\}^{-1}. \tag{9}$$

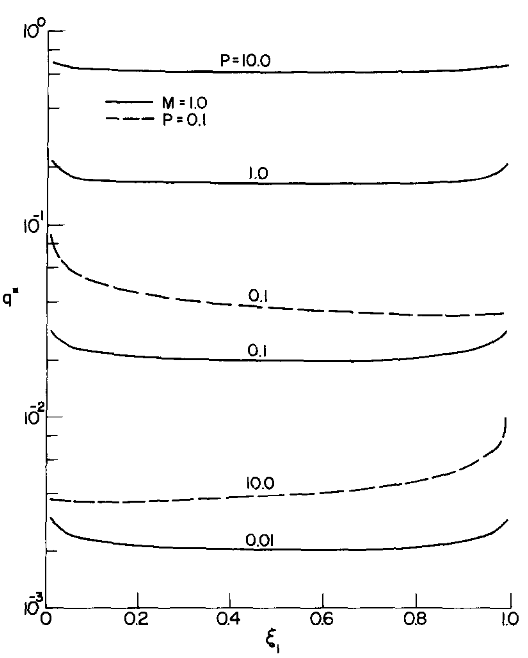

FIG. 3. Effect of parameters P and M on dimensionless heat flux variation along the wall, $Pr_1 = Pr_2 = 0.708$.

As an approximation, the local Nusselt numbers for the uniform wall temperature and uniform heat flux boundary conditions [10] could be used to calculate the heat transfer rate through the wall from equation (9). Unfortunately, neither the wall temperature nor the heat flux are known *a priori*, and an iterative procedure would have to be used.

RESULTS AND DISCUSSION

Dimensionless wall temperature and heat flux

Wall temperature variation along the cold side with air ($Pr_1 = Pr_2 = 0.708$) in both chambers is shown in Fig. 2. The trends in $|\theta_{1w}|$ are similar and are therefore not presented. The limiting case of $P = 0$ corresponds to a plate having no thermal resistance between the two boundary layers. The results for $P = 0.001$ and $P = 0.01$ are very close to those for $P = 0$, and therefore separate curves could not be distinctly indicated. For $M = 1$, an increase in parameter P increases the temperature difference across the wall. Sharp temperature variations are evident from the figure near the bottom and the top of the plate, particularly for small values of P (when $M = 1.0$). For $M < 1$ the resistance to heat transfer on side 2 is much larger than that on side 1, and for $M > 1$ the opposite is true. It is seen from the results given in Fig. 2 that, for $M = 0.1$, about 80% of the temperature drop between the two streams occurs within about 10% of the leading edge.

The dimensionless local heat fluxes corresponding to the wall temperatures just discussed are presented in Fig. 3. If the two fluid streams have the same Prandtl numbers and $M = 1$, the heat flux is symmetrical about the midpoint ($\xi_2 = 1 - \xi_1 = 0.5$) of the plate. Even though the wall temperatures vary significantly with the distance along the wall, the heat flux is practically constant over about 80% of the central height. Only near the top and the bottom of the wall are there relatively large variations in the heat flux. This is due to the fact that the convective heat transfer coefficient at the leading edges of the warm and cold sides of the wall also varies greatly. When the parameter $M \neq 0$ and/or $Pr_1 \neq Pr_2$, the dimensionless heat flux q^* is also not symmetrical about the midpoint of the wall separating the two free convection streams. The more the parameter M departs from unity the greater is the asymmetry in the flux.

The results obtained agree in trends with those available in the literature [6]; however, there are some differences. For example, calculations were performed for $Pr_1 = Pr_2 = 0.72$, $M = 1.0$ and $P = 0.9946$ (corresponding exactly to one of the cases, $\alpha = 1.0$ and $\chi = 0.8$, reported by Lock and Ko [6]), and comparison of plate temperatures has shown that near the ends of the plate Lock and Ko [6] predict more gradual temperature changes than our analysis. Plate temperatures given in Fig. 2 indicate sharp variations near the top and bottom of the test wall. Also, their

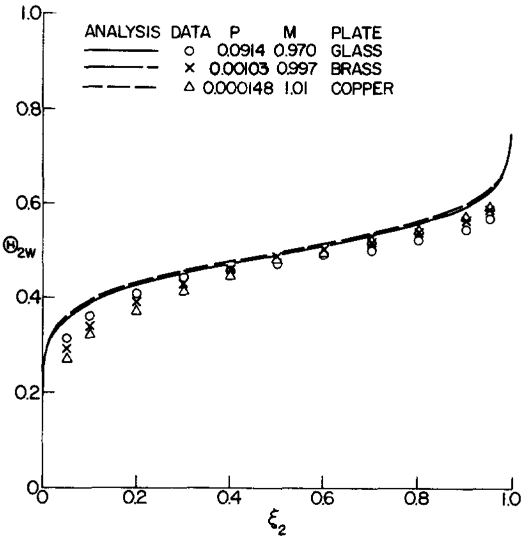

FIG. 4. Comparison of predicted and measured surface temperatures along the wall.

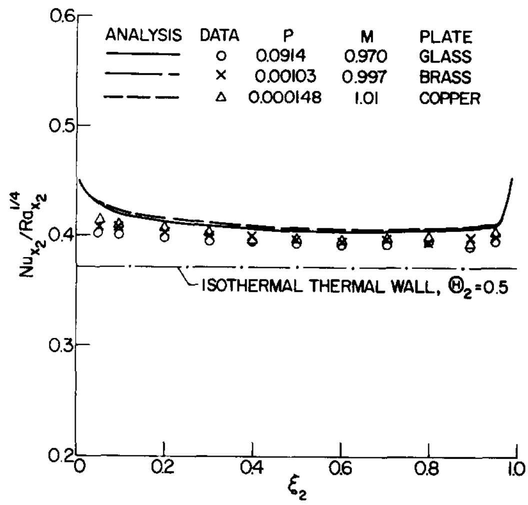

FIG. 5. Comparison of predicted and measured local Nusselt numbers.

calculations yield higher wall temperatures at the top of the cool and at the bottom of the warm sides of the wall than calculated in this work. The discrepancies in predicted temperatures are due to both differences in the formulation and method of solution of the problem. For example, a much finer ($\Delta\xi_1 = 0.01$) grid along the plate was used in obtaining our results. For the average heat transfer parameter $\overline{Nu_L}/Ra^{1/4}$, Lock and Ko [6] obtain a value of 0.209 for $Pr_1 = Pr_2 = 0.72$, $M = 1.0$ and $P = 0.9948$, while the calculations of this work yield a value of 0.174 which is about 17% lower. For the limiting value of $P \to 0$, the two results differ only by about 10%. The discrepancy is attributed primarily to the differences in the method of solution of the model equations. The coupled system of natural convection boundary layer equations for the two streams was solved numerically using an iterative finite difference method [6] and required approximately 30 min of computer time on an IBM 360/67. A finer grid spacing along the plate would have further increased the computational effort. The computations using our method of problem formulation and solution took only about 0.2 s on a CDC 6500 computer for a given case

Comparison of predictions with data

The predicted and measured surface temperatures on the cool side of the wall are compared in Fig. 4. The predictions for the brass plate were very close to those for the copper plate, and therefore for the sake of clarity the curve was not included. The results show that the difference between the calculated and measured surface temperatures is greatest near both the ends. This discrepancy is primarily attributed to the two-dimensional heat conduction effects in the plate. Furthermore, even though the thermal conductivity of the balsa wood was low ($k = 0.055$ W m^{-1} K^{-1}), it is still considerably greater than that of air, and the photographs of the interference fringe patterns clearly showed that there was some heat conducted from the test wall to the wood. Another reason for the discrepancy could be due to the finite size of the two chambers. The natural convection flow established in the chambers in the vicinity of the separating test wall was different from that in an infinite volume of fluid [for which equations (2) and (3) were appropriate].

The local heat-transfer coefficients determined from the local surface minus free stream temperature difference and the local temperature gradient are shown in Fig. 5. The data are presented in a standard form for correlating natural convection heat transfer. The results for an isothermal wall temperature case [10] are also included for the purpose of comparison. Again, the calculated results for the brass plate are not included in the figure for the sake of clarity. The effect of the thermal interaction of the two natural convection systems on local heat transfer is not very significant. The measured natural convection heat-transfer coefficients are a maximum of about 5% lower than the predicted ones and about 12% higher than those expected for a constant temperature wall.

A comparison of predicted and experimentally determined dimensionless heat flux q^* is given in Fig. 6. The approximate analytical results, based on equation (9) (obtained by assuming that there is no interaction between the two natural convection systems across the wall, e.g. taking the wall to be isothermal at $|\theta_{1w}| = \theta_{2w} = 0.5$), are a maximum of about 16% lower than the results based on equation (5). The data points included in the figure were calculated from equation (9) using the experimentally determined Nusselt numbers Nu_{x_1} and Nu_{x_2}. Even

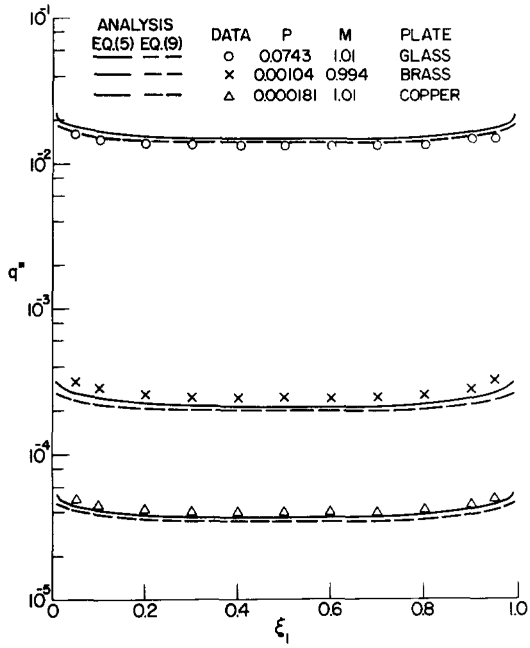

FIG. 6. Comparison of predicted and measured local heat transfer along the wall.

though the heat flux is practically constant over about 80% of the plate height and thus the use of the local Nusselt number correlations for a uniform heat flux boundary condition [10] in evaluating equation (9) would appear to be desirable, it is unknown and therefore prevents direct use of the correlations without iteration. There is a reasonably good agreement between the analytical and experimental results. The largest difference (about 20%) between the predictions of equation (5) and the data is for the brass plate. Since the measured local Nusselt numbers agreed to within about 5% of the predictions, this much greater discrepancy is attributed in larger part to the uncertainty in the thermal conductivity of brass (which is known to be quite sensitive to its precise composition). The conductivity was not measured for the sample, and the value used in the correlation of data was taken from the literature.

CONCLUSIONS

Based on the analytical and experimental results obtained our conclusions are

(1) The natural convection heat transfer coefficients on the two sides of the separating wall are interdependent, but a good agreement for the local heat transfer along the wall can be obtained by neglecting the thermal interaction and using average values of wall temperature and currently accepted procedures in engineering practice, i.e. equation (9).

(2) For ordinary fluids (liquid metals excepted) the thermal interaction between two laminar convection systems separated by a wall is only moderate. Additional experimental and analytical work appears to be warranted for higher thermal conductivity fluids and/or with systems for which two-dimensional heat conduction effects are expected to be more pronounced.

REFERENCES

1. F. Kreith, *Principles of Heat Transfer*, 3rd edn. Intertext Educational, New York (1973). pp. 14–17.
2. R. P. Stein, Liquid metal heat transfer, in *Advances in Heat Transfer*, pp. 101–174, Vol. 3, (edited by T. F. Irvine, Jr. and J. P. Hartnett). Academic Press, New York (1966).
3. R. A. Seban, T. C. Hsieh and R. Greif, Laminar counterflow exchangers: an approximate account of wall resistance and variable transfer coefficients, *J. Heat Transfer* **C94**, 391–396 (1972).
4. R. Viskanta and M. Abrams, Thermal interaction of two streams in boundary layer flow separated by a wall, *Int. J. Heat Mass Transfer* **14**, 1311–1321 (1971).
5. A. Sh. Dorfman, Heat transfer from liquid to liquid in a flow past two sides of a plate, *High Temperature* **8**, 515–520 (1970).
6. G. S. H. Lock and R. S. Ko, Coupling through a wall between two free convective systems, *Int. J. Heat Mass Transfer* **16**, 2087–2096 (1973).
7. C. J. King, The additivity of individual phase resistances in mass transfer operations, *A.I.Ch.E. J.* **10**, 671–677 (1964).
8. W. Hauf and U. Grigull, Optical methods in heat transfer, in *Advances in Heat Transfer*, pp. 133–366, Vol. 6, (edited by J. P. Hartnett and T. F. Irvine, Jr.). Academic Press, New York (1970).
9. G. D. Raithby and K. G. T. Hollands, A general method of obtaining approximate solutions to laminar and turbulent natural convection problems, in *Advances in Heat Transfer*, pp. 265–315, Vol. 11, (edited by T. F. Irvine, Jr. and J. P. Hartnett), Academic Press, New York (1975).
10. S. W. Churchill and H. Ozoe, A correlation for laminar free convection from a vertical plate, *J. Heat Transfer* **C95**, 540–541 (1973).

COUPLAGE DU TRANSFERT THERMIQUE ENTRE DEUX SYSTEMES DE CONVECTION NATURELLE SEPARES PAR UNE PAROI VERTICALE

Résumé—On considère le problème du couplage par conduction à travers un mur qui sépare deux réservoirs de fluides à des températures différentes. On présente une analyse simple pour déterminer le transfert thermique entre deux systèmes de convection séparés par un mur. Des expériences sont effectuées dans un appareil qui permet une observation optique des deux couches limites laminaires avec un interféromètre Mach-Zehnder. On utilise comme fluide d'essai l'air à pression atmosphérique et à température proche de l'ambiance. Un accord raisonnablement bon entre les prévisions et les données expérimentales et obtenu. On montre aussi que la procédure couramment acceptée d'après laquelle est négligée l'interaction thermique entre les deux systèmes de convection naturelle séparés par une paroi, est appropriée pour des fluides ordinaires.

KOPPLUNG DES WÄRMETRANSPORTS ZWISCHEN ZWEI DURCH EINE VERTIKALE WAND GETRENNTEN SYSTEMEN MIT FREIER KONVEKTION

Zusammenfassung—Diese Arbeit befaßt sich mit der thermischen Kopplung durch Wärmeleitung in einer Wand, die zwei Fluidreservoire mit unterschiedlichen Temperaturen trennt. Ein einfaches Berechnungsverfahren für den Wärmetransport zwischen den beiden durch die Wand getrennten Systemen mit freier Konvektion wird angegeben. Es wurden auch Experimente mit einem Versuchsaufbau durchgeführt, bei dem es möglich war, mit Hilfe eines Mach-Zehnder-Interferometers gleichzeitige optische Beobachtungen der beiden laminaren Grenzschichten durchzuführen. Das Versuchsfluid war Luft bei Atmosphärendruck mit einer Temperatur nahe der Raumtemperatur. Dabei wurde eine annehmbar gute Übereinstimmung zwischen rechnerischen Voraussagen und experimentellen Werten erzielt. Es wird auch gezeigt, daß das derzeit übliche Verfahren zur Berechnung des gesamten Wärmedurchgangskoeffizienten mit Vernachlässigung des thermischen Wechselwirkung zwischen den beiden durch eine Wand getrennten Systemen bei freier Konvektion für gewöhnliche Fluide völlig ausreichend ist.

ТЕПЛОВОЕ ВЗАИМОДЕЙСТВИЕ МЕЖДУ ДВУМЯ ЕСТЕСТВЕННО-КОНВЕКТИВНЫМИ СИСТЕМАМИ, РАЗДЕЛЕННЫМИ ВЕРТИКАЛЬНОЙ СТЕНКОЙ

Аннотация — Рассматривается проблема теплового взаимодействия посредством теплопроводности через стенку, разделяющую два заполненных жидкостью резервуара, находящихся при разных температурах. Проведен простой анализ, позволяющий рассчитывать теплообмен между двумя естественно-конвективными системами, разделенными стенкой. Проведены также эксперименты на установке, позволяющей с помощью интерферометра Маха–Цендера проводить оптические наблюдения одновременно за двумя ламинарными пограничными слоями. В качестве рабочей жидкости использовался воздух при атмосферном давлении и комнатной температуре. Получено довольно хорошее совпадение между рассчитанными и экспериментальными данными. Показано, что принятая в настоящее время методика расчета суммарного коэффициента теплообмена, когда пренебрегают тепловым взаимодействием между двумя естественно-конвективными системами, разделенными стенкой, является вполне пригодной для обычных жидкостей.